

Effect of shielding gas on welding performance and properties of duplex and superduplex stainless steel welds

M.A. Valiente Bermejo · L. Karlsson · L.-E. Svensson ·
K. Hurtig · H. Rasmuson · M. Frodigh · P. Bengtsson

Received: 25 July 2014 / Accepted: 13 October 2014 / Published online: 29 October 2014
© International Institute of Welding 2014

Abstract The influence of shielding gases on welding performance and on properties of duplex and superduplex stainless steel welds was studied. Using argon as the reference gas, helium, nitrogen and carbon dioxide were added and five mixtures evaluated. Bead-on-plate welds and circumferential pipe welds were produced using mechanised GMA welding in the downhand position. Welding performance, corrosion resistance, mechanical properties, microstructural features and weld imperfections were assessed and related to the shielding gas. Shielding gases containing 30 % helium showed excellent results; whilst pure argon showed unstable arc and poor weld pool fluidity and Ar+2 %CO₂ resulted in underfill and porosity. Mixtures containing helium resulted in higher ductility welds and higher impact toughness values than welds produced with Ar+2 %CO₂. Sound and balanced duplex microstructures free from intermetallics were found with suitable ferrite contents for all the shielding gases studied. All the duplex pipe welds passed the corrosion test regardless of the shielding gas used, and the best results in the corrosion test for superduplex pipe welds were found when using Ar+30 %He+0.5 %CO₂+1.8 %N₂ as shielding gas.

Keywords Duplex stainless steels · Welding · GMA welding · Shielding gases

1 Introduction

Duplex and superduplex stainless steels are used in several industries and applications where their combination of high strength and superior corrosion resistance are required, for example in oil and gas, transportation, construction and process industries. However, a large-scale application of duplex stainless steels is closely related to the use of welding for fabrication, and it is necessary to find the optimum way to weld these alloys without detriment to their properties. Therefore, the formation of deleterious phases needs to be avoided and a balanced ferrite/austenite microstructure needs to be achieved to meet the required mechanical properties and corrosion resistance [1].

Optimising quality and productivity in welding duplex and superduplex stainless steels is closely related to selecting the optimum shielding gases to get the best properties with a minimum of imperfections. In GMA welding (Gas Metal Arc) there are currently two main groups of shielding gases recommended for welding duplex and superduplex stainless steels: on one hand, argon-based mixtures with small additions of CO₂ or O₂ to help in the arc stabilisation and on the other hand, multicomponent mixtures including argon as the main component and additions of around 30 % helium to improve weld pool fluidity and to allow higher welding speeds and small additions of other gases like CO₂ [1–3]. However, there is some concern about adding nitrogen to the above-mentioned group of shielding gases for GMA welding of duplex and superduplex stainless steels, as it is claimed to increase the risk of porosity [1], whilst nitrogen is commonly added in Gas

Doc. IIW-2511, recommended for publication by Commission IX
“Behaviour of Metals Subjected to Welding.”

M. Valiente Bermejo (✉) · L. Karlsson · L.-E. Svensson · K. Hurtig
Department of Engineering Science, University West,
Gustava Melins Gata, 2, 461 86 Trollhättan, Sweden
e-mail: asun.valiente@hv.se

H. Rasmuson
ESAB AB, 402 77 Göteborg, Sweden

M. Frodigh
Sandvik Materials Technology, 811 81 Sandviken, Sweden

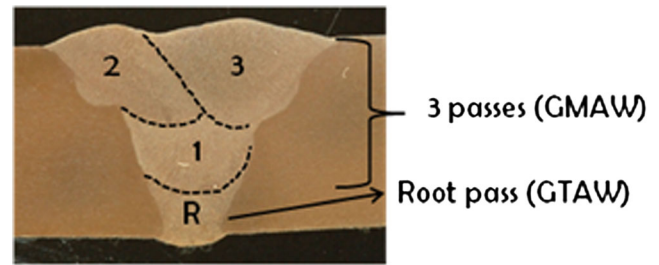
P. Bengtsson
AGA Gas AB, 181 81 Lidingö, Sweden

Table 1 Chemical composition of base materials and filler wires (wt.%)

Material reference	C	Si	Mn	Cr	Ni	Mo	N
SAF 2205 plate	0.021	0.40	1.60	22.0	5.7	3.0	0.17
SAF 2205 pipe	0.017	0.45	0.77	22.4	5.2	3.1	0.17
OK Autrod 2209	0.012	0.48	1.55	23.0	8.6	3.1	0.16
SAF 2507 plate	0.012	0.28	0.80	25.0	6.9	3.8	0.26
SAF 2507 pipe	0.016	0.26	0.47	25.4	6.5	3.9	0.29
OK Autrod 2509	0.014	0.38	0.42	24.1	9.4	3.9	0.22

Tungsten Arc welding (GTA) shielding gases to improve austenite formation and to compensate for possible losses of nitrogen during welding [4]. However, the benefit of nitrogen in the backing gas has been accepted, as it improved the corrosion resistance of the root pass [4, 5].

This research work therefore aims at studying the influence of different shielding gases: argon based but also multicomponent mixtures containing helium, with and without nitrogen, on both corrosion and mechanical properties as well as

**Fig. 1** Multi-pass layout

their influence on welding performance of duplex and superduplex stainless steels.

2 Welding and testing

Duplex stainless steel base material used was type 2205 (W. Nr. 1.4462, UNS S32205, EN X2CrNiMoN 22-5-3) and superduplex stainless steel was type 2507 (W. Nr. 1.4410, UNS S32750, EN X2CrNiMoN 25-7-4). Filler materials employed were OK Autrod 2209 Ø 1 mm

Table 2 Bead-on-plate welds settings

Ref.	Current (A)	Voltage (V)	Arc energy (kJ/mm)	Shielding gas
D 1-1	140	27.0	0.73	Ar+2 %CO ₂
D 1-2	125	24.7	0.61	Ar+2 %CO ₂
D 2-1	140	27.0	0.73	Ar+30 %He+2 %CO ₂
D 2-2	125	24.7	0.61	Ar+30 %He+2 %CO ₂
D 3-1	140	27.0	0.73	Ar
D 3-2	125	24.7	0.61	Ar
SD 4-1	140	27.0	0.76	Ar+2 %CO ₂
SD 4-2	130	24.7	0.64	Ar+2 %CO ₂
SD 4-3	135	27.0	0.73	Ar+2 %CO ₂
SD 4-4	125	24.7	0.61	Ar+2 %CO ₂
SD 5-1	140	27.0	0.76	Ar+30 %He+2 %CO ₂
SD 5-2	130	24.7	0.64	Ar+30 %He+2 %CO ₂
SD 5-3	135	27.0	0.73	Ar+30 %He+2 %CO ₂
SD 5-4	125	24.7	0.61	Ar+30 %He+2 %CO ₂
SD 6-1	140	27.0	0.76	Ar+30 %He+0.5 %CO ₂
SD 6-2	130	24.7	0.64	Ar+30 %He+0.5 %CO ₂
SD 6-3	135	27.0	0.73	Ar+30 %He+0.5 %CO ₂
SD 6-4	125	24.7	0.61	Ar+30 %He+0.5 %CO ₂
SD 7-1	140	27.0	0.76	Ar+30 %He+0.5 %CO ₂ +1.8 %N ₂
SD 7-2	130	24.7	0.64	Ar+30 %He+0.5 %CO ₂ +1.8 %N ₂
SD 7-3	135	27.0	0.73	Ar+30 %He+0.5 %CO ₂ +1.8 %N ₂
SD 7-4	125	24.7	0.61	Ar+30 %He+0.5 %CO ₂ +1.8 %N ₂
SD 8-1	130	24.7	0.64	Ar
SD 8-2	125	24.7	0.61	Ar
SD 8-3	140	27.0	0.76	Ar
SD 8-4	135	27.0	0.73	Ar

Table 3 GMA Welding settings for pipe welds

Sample	Shielding gas	Arc voltage (V)	Current (A)	Welding speed (cm/min)	Arc energy (kJ/mm)
D 1	Ar+2 %CO ₂	25.0	190	27	1.1
D 2	Ar+30 %He+2 %CO ₂	26.5	180	27	1.1
SD 1	Ar+2 %CO ₂	25.0	190	27	1.1
SD 2	Ar+30 %He+0.5 %CO ₂	26.5	180	27	1.1
SD 3	Ar+30 %He+0.5 %CO ₂ + 1.8 %N ₂	26.5	180	27	1.1

(AWS SFA5.9 ER2209, ISO 14343-A G/W 22 9 3 NL) for duplex and OK Autrod 2509 Ø 1 mm (AWS SFA5.9 ER 2594, ISO 14343-A G/W 25 9 4 NL) for superduplex. Table 1 shows the chemical composition of the steels and filler wires.

2.1 Bead-on-plate (BOP) welds

A set of 26 bead-on-plate GMA welds were produced on 20-mm-thickness plates, in downhand welding position (PA according to EN ISO 6947 [6]) and by using 15 l/min shielding gas flow. Plates were cleaned, firstly by mechanical cleaning (machining and grinding the plates) and just before welding plates were also chemically cleaned by ethanol. Three different shielding gases were used for duplex stainless steel welds and each one at two fixed arc energy levels. For superduplex stainless steel welds, five different shielding gases were employed at four different arc energy levels. Table 2 summarises the BOP experiments and settings.

The welding performance of each BOP experiment was assessed in terms of arc stability, weld pool fluidity, bead surface appearance and presence of spatters. Bead profile measurements were taken and the depth/width ratio and dilution were calculated.

2.2 Circumferential pipe welds

Two duplex stainless steel pipes (12 mm thickness, 114 mm OD) and three superduplex stainless steel pipes (12 mm thickness, 118 mm OD) with single-U groove joint preparation were multipass welded. For the root pass, GTA welding was used and pulsed GMA welding was used for the three filling passes in PA position (downhand plus pipe rotation, according to EN ISO 6947 is designated as PA and according to ASME-IX is designated as 1G). Figure 1 shows the multi-pass layout.

The root pass was performed with the same settings for all duplex and superduplex stainless steel pipes: DC GTA welding process in PA position, pure argon as shielding gas (15 l/min), 135 A, 12 V, 6.6 cm/min welding speed. Therefore, 1.5 kJ/mm fixed arc energy, which is in the range of arc energy recommended for duplex and superduplex stainless steel [4, 7, 8]. The only differences between the duplex and superduplex welds were the backing gas used: pure argon (5 l/min) for the duplex and pure nitrogen (5 l/min) for the superduplex welds and also the filler wire: OK Autrod 2209 for duplex and OK Autrod 2509 for superduplex.

For the three GMA welding passes, arc energy was fixed at 1.1 kJ/mm, which was 73 % of the arc energy

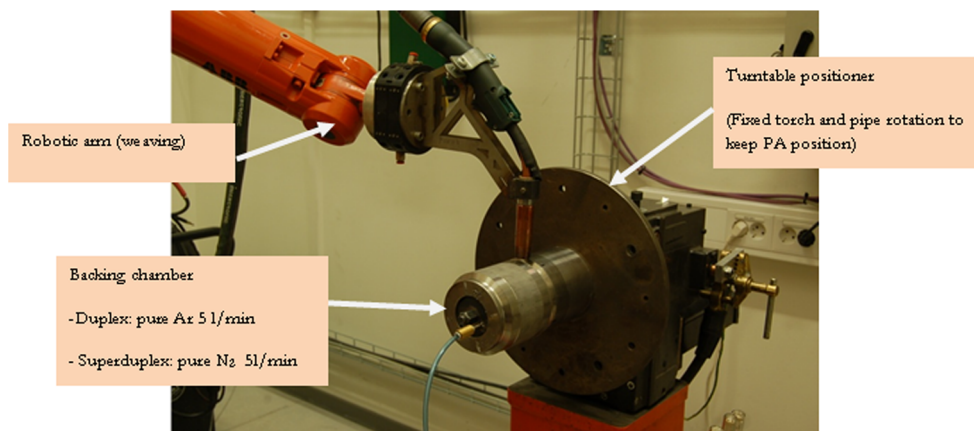
Fig. 2 GMA Welding setup for multi-pass welds

Table 4 Weaving parameters used at each weld pass

Pass	Length of the weave cycle (mm)	Weave width (mm)	Dwell left (mm)	Dwell right (mm)
Root	2	1.9	0.1	0.1
1	4	3.5	0.6	0.6
2	4	5.4	0.3	0.3
3	4	4	0.3	0.3

used in the root pass, as recommended in the literature [1, 4, 7, 8]. Table 3 shows the GMA welding parameters and settings used for the three passes in each experiment to keep the arc energy constant. In those experiments with shielding gases containing helium, it was necessary to reduce the welding current to keep arc energy in the same level as for the mixture Ar+2 %CO₂, due to its higher ionization energy. Figure 2 illustrates the GMA welding setup. Interpass temperature was always lower than 50 °C and grinding between passes was performed to minimise the risk of porosity and lack of fusion of the following pass. Shielding gases were selected according to the results obtained in the previous BOP welds, and it was decided to use these four mixtures: Ar+2 %CO₂, Ar+30 %He+2 %CO₂, Ar+30 %He+0.5 %CO₂, and Ar+30 %He+0.5 %CO₂+1.8 %N₂.

To ensure repeatability in the welding experiments and also with the aim of ensuring a constant welding speed and a constant arc length along the full run length, it was decided to use mechanised welding and to include weaving function in the welding torch. In all cases it was wrist type weaving (similar to the human wrist movement) and a zig-zag weaving shape in the XY plane (the horizontal plane where the weld is produced, but not in the vertical plane). Table 4 shows in full detail the weaving parameters used, which were only dependant on the pass sequence, but not on the shielding gas or the base material.

For a comprehensive characterisation of the pipe welds, the following tests were conducted: macroscopic examination, microstructural inspection, corrosion test (ASTM G48A), cross weld tensile test (ISO 6892–1), Charpy V impact toughness test (EN148-1) of the weld metal and heat affected zone, radiographic test (EN 1435), ferrite measurement (Feritscope: magnetic permeability technique), and chemical analysis.

Different techniques were used for chemical analysis of the welds: high-frequency infrared analysis (HFIR) for C content. Inductively coupled plasma (ICP) for Si, Mn, Cr, Ni and Mo contents and extraction from sample melting by gas fusion analysis (EXTR) was used to determine the O and N contents. Oxygen was analysed

three times by taking three different coupons and average value is reported.

3 Results and discussion

3.1 BOP welds

Welding performance was assessed in terms of arc stability, weld pool fluidity, bead surface appearance and presence of spatters. Each of these four items was rated over 5 points (from 1: very bad, to 5: very good), therefore welding performance was rated over a maximum of 20 points.

Figure 3 depicts the welding performance obtained for the BOP welds using three different shielding gases (pure Ar, Ar+2 %CO₂ and Ar+30 %He+2 %CO₂) in the duplex stainless steel specimens versus the two levels of arc energy studied. From these results, it is clear that both shielding gases containing 2 % CO₂ presented much better welding performance than pure argon and it is also evident that the higher the arc energy, the better welding performance for all the shielding gases used.

Welding performance was also assessed for superduplex stainless steel BOP welds with five different shielding gases (pure Ar, Ar+2 %CO₂, Ar+30 %He+2 %CO₂, Ar+

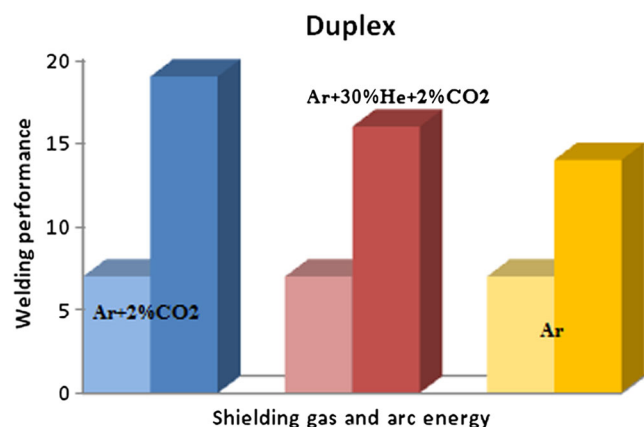
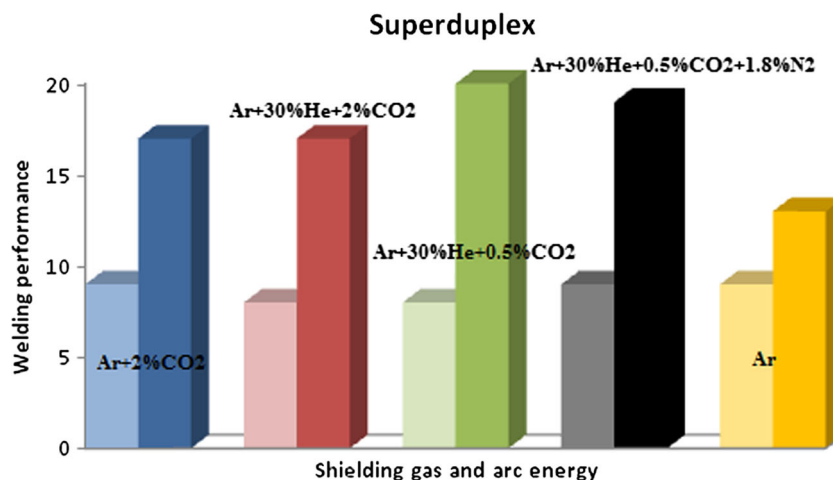


Fig. 3 BOP welding performance in duplex with three shielding gases at two different levels of arc energy. *Left bars*, lower arc energy 0.61 kJ/mm; *right bars*, higher arc energy 0.73 kJ/mm

Fig. 4 BOP welding performance in superduplex with five shielding gases at the highest and lowest levels of arc energy (left bars: 0.61 kJ/mm; right bars: 0.76 kJ/mm)



30 %He+0.5 %CO₂ and Ar+30 %He+0.5 %CO₂+1.8 %N₂) and at four levels of arc energy (0.76 kJ/mm, 0.73 kJ/mm, 0.64 kJ/mm and 0.61 kJ/mm). Figure 4 presents a comparison between the welding performance obtained with the different shielding gases at the highest (0.76 kJ/mm) and the lowest (0.61 kJ/mm) arc energy levels.

Both shielding gases containing 30 % He and 0.5 % CO₂ showed an excellent performance. Similar to results with duplex, for superduplex, all the shielding gases tested resulted in better welding performance than argon. It was also observed that the higher the arc energy, the better welding performance for all the shielding gases as a general trend.

Representative transverse cross-sections of the BOP welds were studied: bead profile dimensions (width, height and penetration, also known as depth) were measured and the parameter depth versus width ratio (D/W) was calculated. Dilution was also calculated from the analysis of the transverse sections as the percentage of the melted base metal area versus the overall transverse area of the bead.

Comparing dilution values at the same arc energy level, when adding CO₂ and/or helium to pure argon, dilution increased, whereas N₂ did not seem to contribute to increased dilution. The higher the percentage of CO₂, the higher the contribution of the base material to the bead, and the presence of both CO₂ and helium in the same gas mixture showed the highest dilution values in the experiments (48 % for superduplex BOP welds and 45 % for duplex BOP welds). Table 5 summarises the results obtained at 0.73 kJ/mm arc energy level. It is well-known that nickel contribution from the filler metal to the weld metal is essential to obtain a balanced duplex microstructure in the weld, therefore making an approximate calculation with the compositions of parent metals and filler metals (Table 1), a contribution around

the 60 % of the filler metal and around the 40 % of the parent metal (dilution) to the weld, would provide a weld metal with a suitable chemical composition to result in a balanced duplex microstructure. As shown in Table 5, dilution values obtained in the experiments with the different gas mixtures are in this range, except for pure argon shielding gas in the superduplex weld, showing only 31 % dilution, which could imply a low penetration weld. Penetration and bead dimensions will be discussed and analysed below.

It is well-known that fluidity of the weld pool for duplex and superduplex stainless steels is lower than for austenitics, and it is also known that the higher nitrogen content in duplex and superduplex in comparison to most austenitics, tends to result in poorer penetrations [7]. These phenomena could increase the risk of lack of fusion in duplex and superduplex stainless steel welds. Therefore, a relatively high D/W value is often desirable and preferable, as it represents a higher penetration. Figure 5 shows the D/W ratio obtained for

Table 5 Dilution versus shielding gas in duplex and superduplex stainless steel BOP welds at the same arc energy level (0.73 kJ/mm)

Ref.	Shielding gas	Dilution (%)
D 1-1	Ar+2 %CO ₂	44
D 2-1	Ar+30 %He+2 %CO ₂	45
D 3-1	Ar	38
SD 4-3	Ar+2 %CO ₂	42
SD 5-3	Ar+30 %He+2 %CO ₂	48
SD 6-3	Ar+30 %He+0.5 %CO ₂	42
SD 7-3	Ar+30 %He+0.5 %CO ₂ +1.8 %N ₂	37
SD 8-4	Ar	31

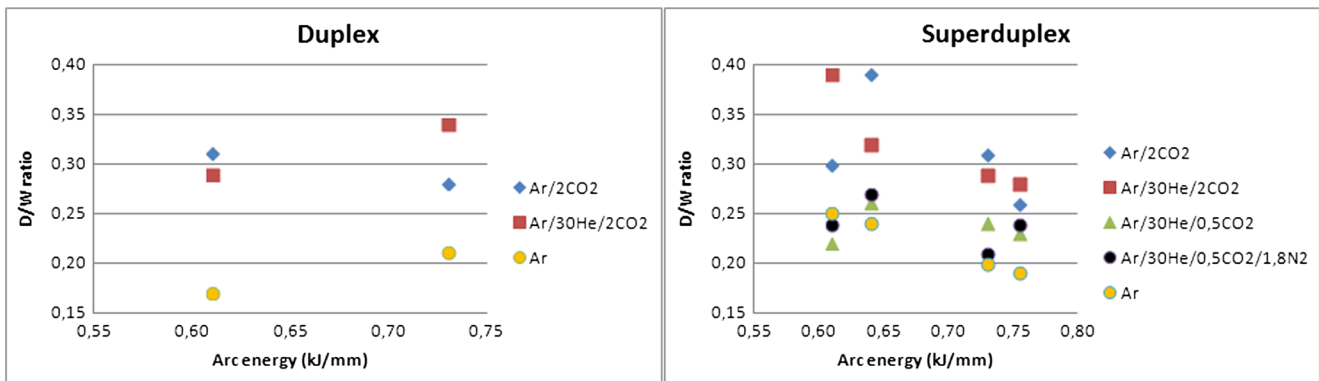


Fig. 5 D/W ratio obtained with different shielding gases at fixed arc energy levels in duplex (*left*) and superduplex (*right*)

the different shielding gases versus the arc energy levels in the duplex and superduplex stainless steel BOP welds. Therefore, from these data it seems clear that both duplex and superduplex stainless steel samples shielded by mixtures containing 2 % CO₂ (Ar+2 %CO₂, Ar+30 %He+2 %CO₂) showed higher D/W values than shielding gases containing only 0.5 % CO₂ (Ar+30 %He+0.5 %CO₂, Ar+30 %He+0.5 %CO₂+1.8 %N₂). This effect could most likely be explained by the influence of oxygen content in the weld pool due to CO₂ decomposition in the arc. Oxygen content influences on the Marangoni convection of the weld pool and it results in narrower and deeper weld profiles [3, 9].

Pure argon showed the lowest D/W ratios, as depicted in Figs. 5 and 6 and also the lowest dilution value, as shown in Table 5. Therefore this gas was rejected for the circumferential pipe welds.

3.2 Circumferential pipe welds

In this chapter, results obtained from the circumferential pipe welds are presented. When discussing all the results it needs to be considered that properties are largely dependent on the thermal cycle and on the chemical composition of the welds. The thermal cycle is kept constant in all the experiments, as arc energy (Table 3) and weaving parameters (Table 4) were equal for all the welds. Differences in properties will be

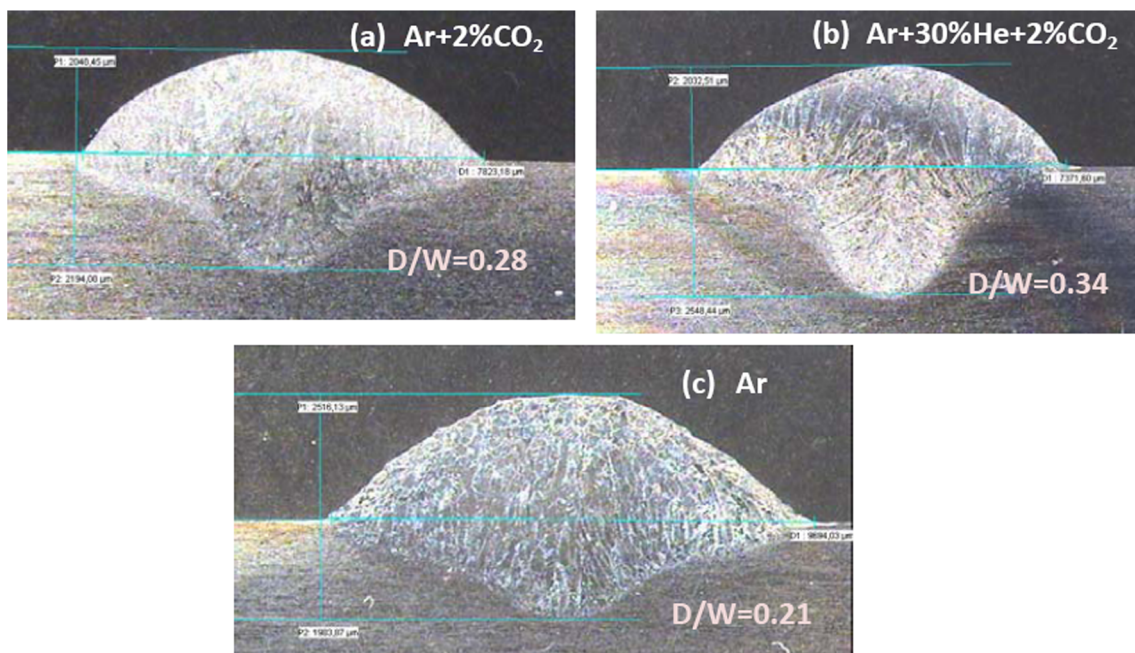


Fig. 6 Duplex bead-on-plate tests conducted with heat input fixed at 0.73 kJ/mm but using different shielding gases. The lowest penetration/width ratio (D/W) is observed when using pure argon

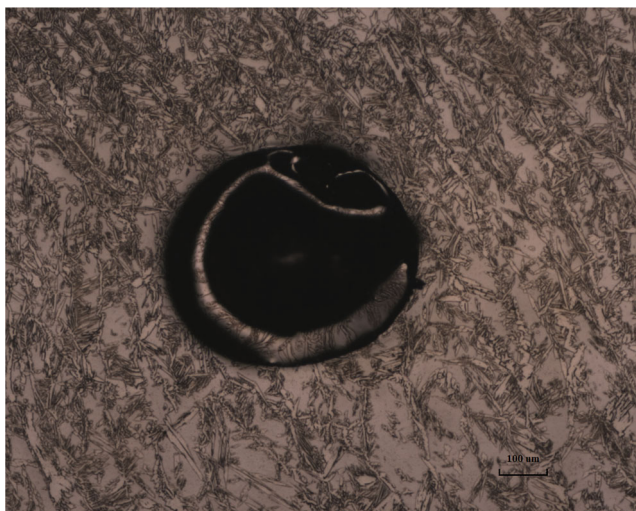


Fig. 7 Transverse cross-section of sample SD 1 shielded by Ar+2 %CO₂ gas and showing porosity

discussed in terms of the variations in chemical composition of the welds caused by the shielding gases.

3.2.1 Weld imperfections: porosity and underfill

Porosity is a common imperfection found in multipass GMA welding of duplex and superduplex stainless steels [7]. This phenomenon could be related to the differences in nitrogen solubility between the molten metal and the solid phases, nitrogen having the highest solubility in austenite phase and the lowest solubility in ferrite phase. Duplex and superduplex stainless steels are nitrogen alloyed (Table 1) for several reasons (austenite-former, corrosion resistance, strengthening element without negative effects on toughness and ductility) and nitrogen is found in solid solution in the base material. However, when duplex material solidifies after welding, its primary solidification mode is ferritic, having the lowest solubility for nitrogen. This can cause a saturation of nitrogen in the liquid and consequently the formation of nitrogen bubbles. It is also known that cleaning the bead surface from oxides between passes in multipass GMA welding of duplex

stainless steels has a positive influence on the reduction of porosity [10].

Porosity was checked by radiographic testing in four specimens per sample according to EN 1435 and porosity was only found when shielding by Ar+2 %CO₂ gas. As a visual example of this phenomenon, the transverse cross-section of sample SD 1 is shown in Fig. 7.

Underfill is a groove weld condition in which the the weld metal surface is below the adjacent surface of the base metal. This irregularity in the weld geometry can be influenced by the surface tension forces in the weld pool, driving the material away from the edges and piling it up along the centre without wetting back the edges properly.

Macroscopic examination was used to inspect the transverse cross section of the specimens. It was found that welds shielded by Ar+2 %CO₂ presented underfill and wider beads than welds shielded by mixtures containing 30 % helium. As shown in Table 3, all the pipe welds with the different shielding gases were produced at the same arc energy value (1.1 kJ/mm), but only those welds shielded by Ar+2 %CO₂ showed underfill (Fig. 8). This fact leads to conclude that the surface tension forces in the weld pool when using Ar+2 %CO₂ shielding gas are different from the surface tension forces of the weld pools obtained when shielding with gas mixtures containing helium.

3.2.2 Chemical analysis

Chemical analysis for welds showed that values are within the standard range for duplex and superduplex stainless steel weld metals (Table 6). However, comparing and contrasting differences in the chemical compositions of the welds obtained with the different shielding gases and considering the chemical compositions of base metals and filler metals (Table 1), it was possible to find some trends.

In the duplex welds, dilution with the parent metal increased when adding helium to the shielding gas, as also happened in the BOP welds (Table 5). Lower contents of nickel in the weld metal when shielding by Ar+30 %He+

Fig. 8 Comparison between bead profiles in superduplex stainless steel welds prepared under the same settings, but only changing shielding gas. *Left:* weld SD 1 shielded by Ar+2 % CO₂ showing underfill. *Right:* weld SD 3 shielded by Ar+30 %He+0.5 %CO₂+1.8 %N₂ free from underfill

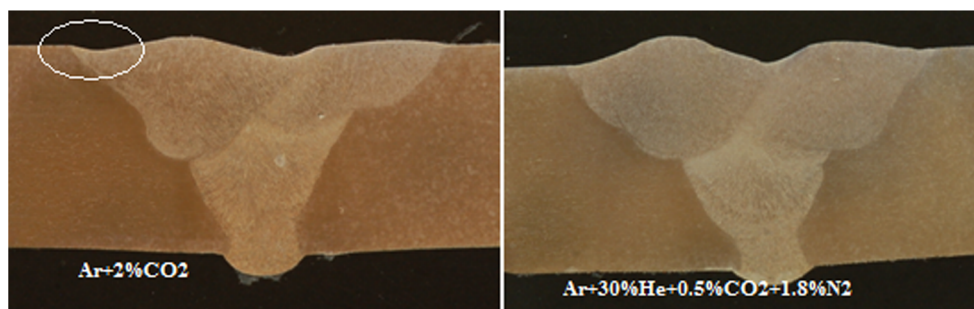


Table 6 Chemical analysis of the weld metals (wt.%)

Sample	Shielding gas	C	Si	Mn	Cr	Ni	Mo	O (ppm)	N
D 1	Ar/2CO ₂	0.020	0.47	1.31	23.2	8.9	3.01	227	0.15
D 2	Ar/30He/2CO ₂	0.020	0.47	1.30	21.8	8.4	2.86	439	0.15
SD 1	Ar/2CO ₂	0.024	0.36	0.41	25.2	9.4	3.74	309	0.23
SD 2	Ar/30He/0.5CO ₂	0.017	0.34	0.41	24.8	9.7	3.70	148	0.22
SD 3	Ar/30He/0.5CO ₂ /1.8 N ₂	0.017	0.35	0.40	25.1	9.6	3.71	125	0.24

2 %CO₂ denoted lower contribution of the filler metal to the weld and higher dilution with the duplex base material.

In the superduplex welds, the dilution effect with the main alloying elements is not clear, but it was found a decrease in the carbon and the oxygen contents in the weld metal when reducing CO₂ content and increasing N₂ content in the shielding gas.

Regarding the nitrogen content of the weld metal, in the duplex welds it did not seem to be influenced by the addition of helium in the shielding gas. In the superduplex welds, the differences in helium and CO₂ contents in the shielding gases did not result in a significant difference on the nitrogen content of the weld metal. However, as it was foreseeable, the highest nitrogen content is found in the weld shielded by the shielding gas mixture containing an addition of N₂.

Regarding the oxygen content in the weld metal, it was found that those welds shielded with 2 %CO₂ content showed higher oxygen contents than those shielded with 0.5 %CO₂ mixtures. Some authors found that the active gas CO₂ can be decomposed in the arc and resulting oxygen dissolved in the weld pool [3, 9]. Therefore, it would be expected to find higher oxygen contents in the weld metal when using higher contents

of active gas in the shielding mixture. As it will be discussed in the corrosion chapter later on, this phenomenon could have had an influence on the corrosion resistance results of superduplex welds, and maybe it could even be related to the previously discussed underfill found in the samples shielded with Ar+2 %CO₂.

3.2.3 Mechanical testing

Tensile test (in accordance with ISO 6892–1) and Charpy impact toughness test (in accordance with EN 148–1) were conducted on the specimens. Results are summarized in Table 7.

All the specimens passed the Charpy-V impact toughness testing in the WM (weld metal) and in the HAZ (heat affected zone) at –40 °C as all exceeded the common minimum requirements with absorbed energy values exceeding 27 and 47 J [11, 12]. Regarding cross tensile test, all the specimens showed yield strength values and ultimate tensile strength values higher than the minimum values required for the base metals (R_{p 0.2}>485 MPa and R_m 680–880 MPa for 2205 and R_{p 0.2}>550 MPa and R_m 800–1,000 MPa for 2507) and in all cases fracture took place in the base material.

Table 7 Summary of mechanical test results

Sample	Shielding gas	Impact toughness –40 °C, (J), 3 tests						Cross weld tensile testing, 2 tests			
		WM min	WM max	WM av.	HAZ min	HAZ max	HAZ av.	R _{p 0.2} (MPa)	R _m (MPa)	A (%) Elongation	Z (%) Area reduction
D 1	Ar/2CO ₂	125	176	152	202	234	218	589	774	15.0	72.0
								613	778	16.4	72.0
D 2	Ar/30He/2CO ₂	194	208	202	190	211	200	599	773	27.1	71.0
								606	769	25.3	72.0
SD 1	Ar/2CO ₂	164	180	174	145	170	154	644	834	20.0	76.0
								642	839	25.9	75.0
SD 2	Ar/30He/0.5CO ₂	185	211	194	152	199	175	647	843	30.7	76.0
								651	844	32.2	77.0
SD 3	Ar/30He/0.5CO ₂ /1.8 N ₂	150	179	160	223	227	225	644	839	33.2	77.0
								639	829	20.8	75.0

Table 8 Corrosion test results

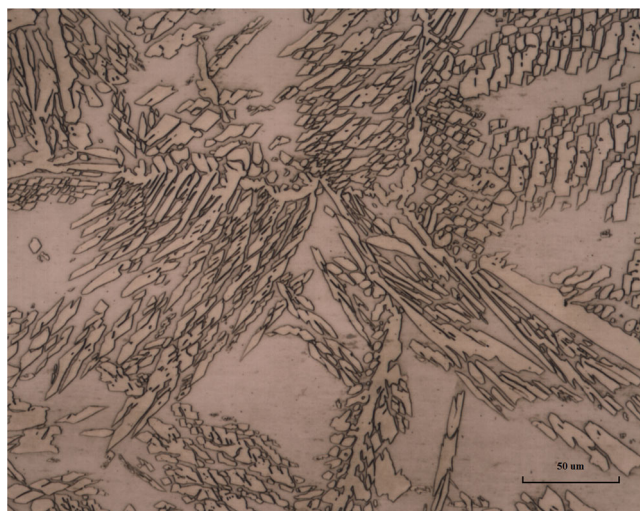
Sample	Shielding gas	T (°C)	Weight loss (g/m ²)	Comment
D 1	Ar/2CO ₂	20	0.2376	Acceptable
		20	0.1446	Acceptable
D 2	Ar/30He/2CO ₂	20	0.1628	Acceptable
		20	0.2710	Acceptable
SD 1	Ar/2CO ₂	40	2.6016	Not acceptable
		40	1.8000	Not acceptable
SD 2	Ar/30He/0.5CO ₂	40	0.5514	Acceptable
		40	1.0302	Not acceptable
SD 3	Ar/30He/0.5CO ₂ /1.8 N ₂	40	0.6436	Acceptable
		40	0.7073	Acceptable

In duplex and superduplex welds, it is noticeable that when adding helium to the shielding gas, ductility values increased in comparison to ductility in welds shielded by Ar+2 %CO₂, and the same trend is observed when comparing impact toughness values.

3.2.4 Corrosion test and microstructural inspection

Pitting corrosion susceptibility was evaluated for two samples per weld in accordance with ASTM G48A. Testing time was 24 h and testing temperature was 20 °C for duplex and 40 °C for superduplex. It was established as acceptance criterion 1 g/m² as the maximum weight loss.

As shown in Table 8, all the duplex samples passed the corrosion test at 20 °C regardless of the shielding gas used. This fits very well with the microstructural inspection conducted on these corrosion tested samples, as both presented a sound duplex microstructure free from intermetallics (Fig. 9).

**Fig. 9** Sound duplex microstructure in D1 sample

Regarding superduplex samples, both SD 3 specimens shielded by Ar+30 %He+0.5 %CO₂+1.8 %N₂ passed the test whilst both SD 1 specimens shielded by Ar+2 %CO₂ failed to meet the requirements. When comparing the chemical composition of these welds (Table 6), the higher nitrogen content and the lower oxygen content of SD 3 specimens could explain the better corrosion results when shielding by Ar+30 %He+0.5 %CO₂+1.8 %N₂. If the acceptance criterion of 4 g/m² for superduplex 2507 proposed by NORSOK standard [12] had been considered, then all the superduplex samples would have passed the test.

In any case, when inspecting the transverse cross sections of the not acceptable specimens due to weight loss criterion, no pitting corrosion or intermetallics were observed. Instead, they showed a typical duplex microstructure with some secondary austenite (Fig. 10); however, it was not found in significant amounts and it was located in isolated areas, therefore it would not be necessarily harmful for the material properties.

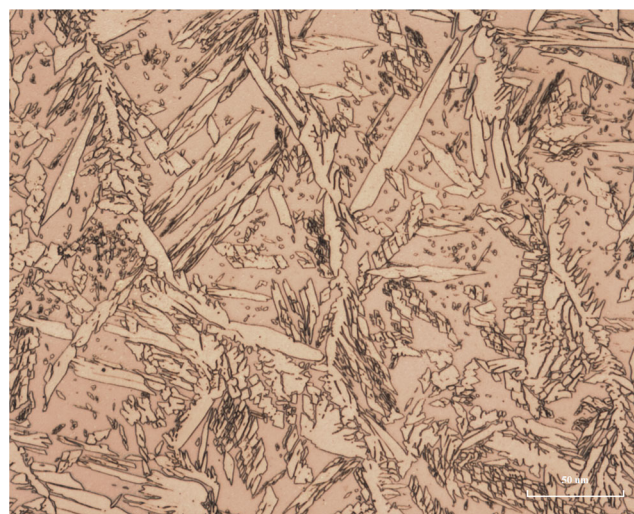
**Fig. 10** Some secondary austenite between the second and third pass boundary in SD 2 specimen

Table 9 Ferrite contents determined by Feritscope

Sample	Pass 1				Pass 2				Pass 3				Av. WM	Base Material			
	FN	s	Min	Max	FN	s	Min	Max	FN	s	Min	Max	FN	FN	s	Min	Max
D 1	61	1	60	62	68	2	65	70	71	4	67	77	67	71	8	63	82
D 2	65	1	64	67	67	1	64	68	70	2	68	72	67	73	5	67	79
SD 1	56	2	52	58	56	2	52	58	58	2	55	60	57	56	3	52	60
SD 2	58	2	55	59	59	2	56	61	59	2	57	61	59	52	2	50	55
SD 3	59	2	57	62	60	1	58	61	63	1	63	64	61	52	1	51	53

s standard deviation

3.2.5 Ferrite content

Duplex stainless steel base materials are usually supplied in solution-annealed state with a balanced microstructure of around 50 % ferrite and 50 % austenite. After welding, they experience a primary ferritic solidification mode, and once solidification finishes, ferrite transforms to austenite through a solid-state-phase transformation. However, cooling after welding is too rapid to permit the austenite content to approach equilibrium levels. Therefore, to have a balanced duplex microstructure in the weld metal, filler metals are over-alloyed with nickel to stabilize austenite. In addition to heat input and cooling rate conditions, in multipass welds, ferrite content is also influenced by dilution, so the typical ferrite content in duplex and superduplex widely depends on welding conditions, and could be approximately in the range between 30 and 70 % [2, 7, 8, 13].

Ferrite content was measured in the transverse cross section of the samples by using a calibrated Fischer Feritscope FMP30. Five individual measurements were taken at each weld pass, paying attention to cover the area but staying around 1.5 mm away from the edges and from the rest of passes to avoid interferences. The average ferrite content for each weld pass, but also the average content for the whole weld metal (calculated from 15 measurements=5 measurements per pass×3 passes) and the ferrite content of the base material are

presented in Table 9. These results showed average ferrite content, for each weld pass as well as the average content for the whole weld metal, fully in accordance with a balanced ferrite/austenite microstructure in all the samples.

It is not possible to observe significant differences in the experimental ferrite contents of the welds in relation to the different shielding gases used. When trying to correlate chemical compositions of the weld metals (Table 6) and experimental ferrite contents, it was expected that those welds shielded by helium mixtures showed slightly lower ferrite contents than welds shielded by Ar+2 %CO₂ as chromium content in welds shielded by helium mixtures were slightly lower. However, that behaviour was not observed in the experimental measurements, but the phenomenon was observed when the chemical composition of the welds was used to predict ferrite contents using the FNN-1999 artificial neural network proposed by Vitek et al. [14], the WRC-1992 proposed by Kotecki et al. [15] and the mathematical regression proposed by Valiente [16], as shown in Table 10. These previous models refer to single pass or last pass ferrite contents and they do not consider reheating effects. That could explain the differences found between the experimental and the predicted values, however, it is noticeable that Valiente's regression predicts ferrite contents closer to the experimental values than the other methods.

Table 10 Comparison between experimental and calculated ferrite content (FN)

Sample	Shielding gas	Experimental	FNN-1999	WRC-1992	Valiente
D 1	Ar/2CO ₂	67	41	50	55
D 2	Ar/30He/2CO ₂	67	35	38	46
SD 1	Ar/2CO ₂	57	48	50	65
SD 2	Ar/30He/0.5CO ₂	59	43	48	61
SD 3	Ar/30He/0.5CO ₂ /1.8 N ₂	61	44	48	62

4 Conclusions

Five shielding gases were evaluated: pure Ar, Ar+2 %CO₂, Ar+30 %He+2 %CO₂, Ar+30 %He+0.5 %CO₂ and Ar+30 %He+0.5 %CO₂+1.8 %N₂. It was found that shielding gas composition influences the welding performance and the chemical composition of the weld metal and consequently differences in properties were observed.

Both shielding gases containing 30 % He and 0.5 % CO₂ showed excellent arc stability, weld pool fluidity, smooth bead profile and absence of spatter, whilst pure argon showed less good behaviour. It was also observed that the higher the arc energy, the better welding performance for all the shielding gases as a general trend.

When adding CO₂ and/or helium to pure argon in the shielding gas, dilution with the base material increased. The presence of both CO₂ and helium in the same gas mixture showed the highest dilution.

No weld imperfections were found in the pipe welds shielded by mixtures containing helium, whilst porosity and underfill were found in welds shielded by Ar+2 %CO₂.

High-quality welds showing high ductility, excellent impact toughness values, sound microstructure and good corrosion resistance were produced in duplex and superduplex stainless steel pipes in downhand position using shielding gases with 30 % helium.

From the five gas mixtures evaluated, best results were obtained with the three multicomponent mixtures containing Ar–30 %He, and no significant differences in weld metal properties were found among those three mixtures. Therefore, the final criteria to select the specific Ar–30 %He shielding gas for welding duplex and superduplex stainless steels can be based on price and availability.

Acknowledgments The Knowledge Foundation is gratefully acknowledged for the economic funding. The great support received from the business partners involved: AGA Gas AB, ESAB AB and Sandvik Materials Technology and the involvement and contribution of their representatives are also acknowledged.

References

- Karlsson L (2012) Welding duplex stainless steels—a current review of recommendations. *Weld World* 56:65–76
- van Nassau L, Meelker H, Hilkes J (1993) Welding duplex and superduplex stainless steels. *Weld World* 31(5):322–343
- Lu S, Fujii H, Nogi K (2010) Weld shape variation and electrode oxidation behavior under Ar-(Ar-CO₂) double shielded GTA welding. *J Mat Sci Technol* 26(2):170–176
- Pettersson C-O, Fager S-Å (1995) Welding practice for the Sandvik duplex stainless steels SAF 2304, SAF 2205 and SAF 2507. AB Sandvik Steel. Technical document S-91-57, 15
- Westin EM, Johansson MM, Bylund L-Å, Pettersson RFA (2013) Effect on microstructure and properties of superduplex stainless steel welds when using backing gas containing nitrogen and hydrogen. IIW Commission IX Document IX-2459-13 rev.1. 9
- EN ISO 6947:2011 (2011) Welding and allied processes—welding positions
- How to weld duplex stainless steels (2006) Avesta Welding AB. Document 10601EN-GB, Avesta, Sweden, 20
- Welding guidelines for duplex & superduplex stainless steels (2005) Metrode Products Limited. Chertsey, UK, 7
- Fuji H, Lu S, Sato T, Nogi K (2008) Effect of oxygen content in He-O₂ shielding gas on weld shape for ultra deep penetration TIG. *Trans Jpn Weld Res Inst* 37(1):19–26
- Persson K-A (2014) Pore formation in MIG welding duplex stainless steels with super duplex filler wire. Conference “Svetsning av rostfria stål” organised by Swerea/Kimab. Stockholm
- EN 10028: 2008 (2008) Flat products made of steels for pressure purposes, part 7: stainless steels
- NORSOK STANDARD M-601 (2008) Welding and inspection of piping
- Welding consumables technical handbook (2009) Metrode Products Limited. Revision 10, Chertsey, UK, 384
- Vitek JM, Iskander YS, Oblow EM (2000) Improved ferrite number prediction in stainless steel arc welds using artificial neural networks—part 2: neural network results. *Weld J* 79(2): 41s–50s
- Kotecki DJ, Siewert TA (1992) WRC-1992 constitution diagram for stainless steel weld metals: a modification of the WRC-1988 diagram. *Weld J* 71(5):171s–178s
- Valiente-Bermejo MA (2012) A mathematical model to predict δ-ferrite content in austenitic stainless steel weld metals. *Weld World* 56(09–10):48–68